

SHAPE IDENTIFICATION OF A 3-D WELD POOL BY USING BEZIER SURFACES

Duc Dung DOAN⁽¹⁾, Franck GABRIEL⁽²⁾, Yvon JARNY⁽³⁾, Philippe LE MASSON⁽⁴⁾.

⁽¹⁾ Atomic Energy Agency, Bât. 611 CEA Saclay CEA\DR\DTEN\LITEN\UTIAC, 91191 Gif sur Yvette Cedex, France,
Email: duc-dung.doan@cea.fr

⁽²⁾ Atomic Energy Agency, Bât. 470 CEA Saclay CEA\DTEN\DM2S\SERMA, 91191 Gif sur Yvette Cedex, France,
Email: franck.gabriel@cea.fr

⁽³⁾ Heat transfer Laboratory, UMR CNRS 6607, University of Nantes, Polytech'Nantes Site de Chantrerie, BP 50609,
44306 Nantes Cedex 3, France, Email: yvon.jarny@polytech.univ-nantes.fr

⁽⁴⁾ LET2E University of South Brittany, Rue de Saint Maudé, BP 92116, 56321 Lorient Cedex, France,
Email: philippe.le-masson@univ-ubs.fr

ABSTRACT

The paper deals with the heat transfer analysis in a welding process: a method is developed to determine the shape of the 3-D phase change front and to estimate the temperature field within the solid part of the work piece. The problem is formulated and solved as an inverse phase-change problem by using an optimisation method. The direct problem is solved in the torch frame and so formulated as an eulerian approach. The interface between the weld pool and the solid region is parameterised by Bezier surfaces.

The most important feature of the presented approach is that the liquid-solid interface as well as the temperature distribution within the solid region can be obtained from additional temperature data available in the solid region, without considering heat transfer and fluid flow in a molten zone. The estimate of these thermal characteristics allows then a thermomechanical calculation of the welded joint (calculation of the deformations and residual stresses). The validity of the numerical solution of the inverse problem is checked by comparing the results with the direct solution of the problem.

Keywords: Bezier surface, Front of fusion, Heat source, Welding, Inverse method.

1. NOMENCLATURE

λ_s : Thermal conductivity of the Solid
 ρ_s : Density of the Solid
 c : Heat capacity
 u : Torch velocity
 Γ : Liquid-Solid interface
 Ω_s : Solid domain
 T_s : Temperature within the solid domain
 T_e : Exterior temperature
 T_{imp} : Imposed temperature
 T_f : Melting temperature
 h : Overall heat transfer coefficient

e : Thickness of the work piece

M : Number of points of measurement

Y^m : Temperature measurement at sensors location

2. INTRODUCTION

Welding is a complex process that involves many parameters that may have important influences on the final solidification structure and the properties of the welded joint [1]. During the welding process, the edge of two pieces of metal are melted and fused together. This is done using an intense local energy source. Transmitted energy causes the fusion of metal as well as the creation of a molten pool usually referred to as a weld pool. It is important to be able to control the size and shape of the weld pool [2]. It must be small enough to be manageable and minimize energy consumption but large enough to bond the two pieces properly.

Studies that deal with the inverse technique for the analysis of melting and solidification processes are limited. Earlier efforts have focused on one dimensional problem [3-5]. The literature includes the two-dimensional stationary arc welding problem in which Hsu uses transient temperature data from thermocouples imbedded in the solid region to determine through a Newton-Raphson interpolation procedure the transient position of the liquid-solid interface and the transient temperature distribution in the solid region [9]. Later, it includes the two-dimensional design problem [7], [8] and the two-dimensional inverse geometry problem in continuous casting of metals [9]. Recently, D.D. Doan and al. have developed an original method to identify the position and the shape of a 2-D melting pool using the parameterisation by Bezier splines [11] [14].

This work focuses on the application of the inverse technique and Bezier surfaces for identifying the location of the 3D liquid-solid interface. Furthermore it can be noted that in quasi steady state, the

determination of the heat flux crossing this interface results directly from the knowledge of both the front location and the temperature field within the solid region.

3. PROBLEM STATEMENT

3.1 The Welding Process

The phase-change phenomenon is considered in the following experimental conditions (Figure 1). A welding arc having a power of sufficient intensity moves with a constant velocity (axis x) and strikes the edge of two metal plates. A weld pool is formed and moves at the same velocity as the welding arc.

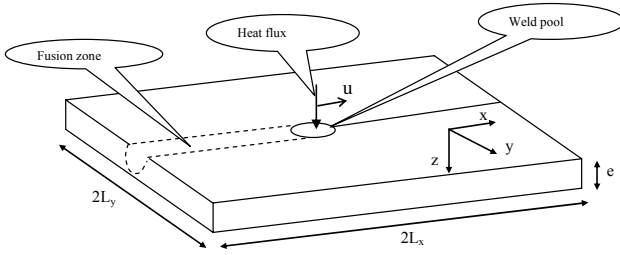


Figure 1 Schematic diagram of welding process

The mathematical representation of the problem includes the following physical processes and other general assumptions and conditions:

1. The heat transfer between two plates during the welding process when the welding torch moves with a constant velocity is unsteady in a fixed coordinate system. A quasi-steady-state problem can be achieved in a coordinate system that moves with the heat source. Thus, a moving coordinate system is used for the analysis of the inverse problem. This means that the size of the weld pool under the welding arc is constant while the material enters and leaves the computational domain.
2. In quasi-steady-state, to obtain the shape of the weld pool and the temperature field in the solid domain, we formulate and solve the heat conduction problem within the solid region by considering the melting temperature as the imposed temperature at the liquid-solid interface.
3. The Bézier surface with its control points is used to define the position of the liquid-solid interface. In this work, this assumption is used in order to form the initial position of the liquid-solid interface and to create a numerical experiment, i.e., the temperature data at the points of measurement located within the solid region. The location of the sensors is

constant with respect to the moving coordinate.

3.2 Modelling Equations

The modelling equations which determine the temperature field within the solid region consist on the energy equation (1) with a moving heat source along the x axis, together with adiabatic conditions on the boundaries and a symmetric condition (2), the condition at the top and the bottom of the work piece (3) (4), the imposed temperature on the boundary at $x = L_2$ and the specification of the melting temperature along the phase change front (5).

$$\rho_s c_s u \frac{\partial T_s(x, y, z)}{\partial x} = \nabla[\lambda_s \nabla T_s(x, y, z)] \quad (x, y, z) \in \Omega_s \quad (1)$$

$$\frac{\partial T_s}{\partial y} = 0 \text{ at } y = L_y; \frac{\partial T_s}{\partial x} = 0 \text{ at } x = -L_1 \text{ and } \frac{\partial T_s}{\partial y} = 0 \text{ at } y = 0 \quad (2)$$

$$-\lambda_s \frac{\partial T(x, y, z_0)}{\partial z} + hT(x, y, z_0) = hT_e \text{ at } z = z_0 = 0 \quad (3)$$

$$\lambda_s \frac{\partial T(x, y, z_{ep})}{\partial z} + hT(x, y, z_{ep}) = hT_e \text{ at } z = z_{ep} = e \quad (4)$$

$$T = T_{mp} \text{ at } x = +L_2, T(x, y, z) = T_f \text{ at } (x, y, z) \in \Gamma \quad (5)$$

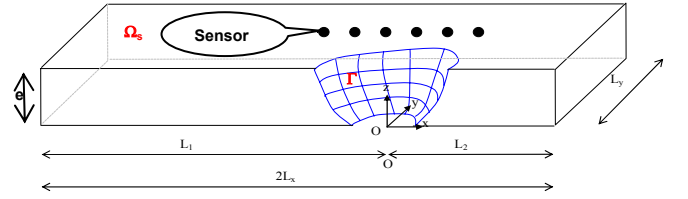


Figure 2 Schematic of spatial domain

The shape Γ of the isothermal phase change front has to be determined. Considering a heat flux balance equation to determine this shape is non practicable because no experimental data are available to characterize the heat flux distribution lost by the weld pool through this front. Therefore the shape of the front will be determined using an inverse approach which needs additional data given by the temperature measurements at M points located in the solid region:

$$T(x_m, y_m, z_m) = Y^m \quad m = 1, 2, \dots, M \quad (x, y, z) \in \Omega_s \quad (6)$$

Hence the inverse problem, considered of interest here, aims the shape Γ identification of the phase change front and the estimation of the temperature field within the solid part Ω_s of the work piece for the modelling equations (1)-(6). The main difficulty in the resolution of this kind of problem comes from its ill-posed nature. That is why the measurement sensor number should be

appropriate to make the problem over-determined, or at least must be equal to the number of design variables. Thus, in general, inverse analysis leads to optimization procedures of an objective function $S(X)$ of the least squares type built with $T(x_m, y_m, z_m; \Gamma)$ the predicted temperatures by the modelling equation (1)-(5), Γ being fixed, and the measured temperatures, equation (6). The inverse phase change problem is formulated as an optimization problem, it consists in: Finding Γ which minimizes:

$$S(\Gamma) = \frac{1}{M} \sum_{m=1}^M (T(x_m, y_m, z_m; \Gamma) - Y^m)^2 \quad (7)$$

Then the inverse analysis is performed without solving heat transfer and fluid flow equations in the liquid region. The idea of the iterative algorithm is as follows:

- Step 1: Choose an initial guess of the shape Γ and its parameterisation by Bezier surface (see next section).
- Step 2: Compute the sensitivity of the predicted temperature at the sensor locations with respect to the vector parameter X of Bezier surface, defined by the coordinates of the control points.
- Step 3: Use the Levenberg-Marquardt algorithm [10] to correct the vector parameter X .
- Step 4: Repeat the procedure until convergence is achieved.

Modelling of phase change processes requires smooth curves representing phase change fronts. Nehad Al-Khadily [7] describes the phase change boundary with a two-dimensional coordinate system assumed in the molten zone. Each point at the phase change boundary is located by its radial and angular coordinates, i.e., radial distance from the keyhole center and the angular direction. Since the interface location is just a guess, the obtained temperature profile through the work piece will differ from the exact. The exact location of the liquid-solid interface as well as the temperature profile is found by use of the prediction-correction method. Choice of the number of nodes to form the interface plays a major role in obtaining accurate and efficient solution of the inverse problem. However, when the shape of the phase change fronts is complex this number of nodes is important i.e. more measurement sensors are needed. As noticed before, the ill-posed nature of all inverse problems requires making them over-determined by performing an appropriate number of measurements. On the other hand, it is very important to limit the number of sensors because of commonly known difficulties with data acquisition. Furthermore, each measurement introduces not only variable information but also some noise. Application of Bezier surface permits to parameterize the phase change front using a smaller

number of parameters and, consequently, reduce the number of sensors.

3.3 Parameterisation of the front Γ by Bezier Surfaces

Generally, the Bezier surface is formulated as follows:

$$P(u, v) = \sum_{i=0}^m \sum_{j=0}^n B_i^m(u) B_j^n(v) P_{ij} \quad \text{with } u \in [0, 1], v \in [0, 1]$$

$$B_i^m(u) = \frac{m!}{i!(m-i)!} u^i (1-u)^{m-i} \quad (8)$$

$$B_j^n(v) = \frac{n!}{j!(n-j)!} v^j (1-v)^{n-j}$$

where $P(u, v)$ stands for any point on the Bézier surface, P_{ij} is the control point, $m \times n$ is the degree of Bézier surface, $N = (m+1) \times (n+1)$ is the number of control point, u and v vary in the range $[0, 1]$ and $B_i^m(u)$, $B_j^n(v)$ are the Bernstein polynomials.

The majority of weld pool interfaces can be represented by cubic Bézier surface (with $m = 2, n = 3$). Such curves are based on twelve control points $P_0, P_1, P_2, \dots, P_{12}$ (Fig. 3) as presented in the following formulation.

$$P(u, v) = \sum_{i=0}^2 \sum_{j=0}^3 P_{ij} \frac{2!}{i!(2-i)!} u^i (1-u)^{2-i} \frac{3!}{j!(3-j)!} v^j (1-v)^{3-j}$$

$$= P_{00} (1-u)^2 (1-v)^3 + P_{01} (1-u)^2 3v(1-v)^2$$

$$+ P_{02} (1-u)^2 3v^2(1-v) + P_{03} (1-u)^2 v^3$$

$$+ P_{10} 2u(1-u)(1-v)^3 + P_{11} 2u(1-u)3v(1-v)^2$$

$$+ P_{12} 2u(1-u)3v^2(1-v) + P_{13} 2u(1-u)v^3$$

$$+ P_{20} u^2(1-v)^3 + P_{21} u^2 3v(1-v)^2 + P_{22} u^2 3v^2(1-v)$$

$$+ P_{23} u^2 v^3$$

with $u \in [0, 1]; v \in [0, 1]$ (9)

This means that the shape of the interface Γ is described by twelve control points (i.e. thirty six coordinates in the 3-D case). The proposed approach has a number of important advantages. First of all, the application of Bezier surface of degree (2×3) ensures smoothness of the phase change front. The next very important advantage is that this application permits to limit the size of the vector parameter X to be identified. In practice, some coordinates of the Bezier control points are defined by additional conditions resulting from the physical nature of the problem. In the case studied here the coordinates of $P_{20}, P_{23}, P_{00}, P_{03}$ are assumed to be given and the following coordinates

$P_{00y} = P_{10y} = P_{20y} = P_{30y} = P_{03y} = P_{13y} = P_{23y}$ can be taken equal to zero.

In the other hand, by using the symmetry condition, we have $P_{21x} = P_{20x}, P_{22x} = P_{23x}, P_{01x} = P_{00x}, P_{02x} = P_{03x},$

$P_{11x} = P_{10x}, P_{12x} = P_{13x}$. We impose

$$P_{10z} = P_{11z} = P_{12z} = P_{13z}$$

Finally, the size of the vector parameter X is limited to nine: $\dim(X) = 9$ with

$$X = [P_{01y}, P_{02y}, P_{10x}, P_{13x}, P_{11y}, P_{12y}, P_{10z}, P_{21y}, P_{22y}].$$

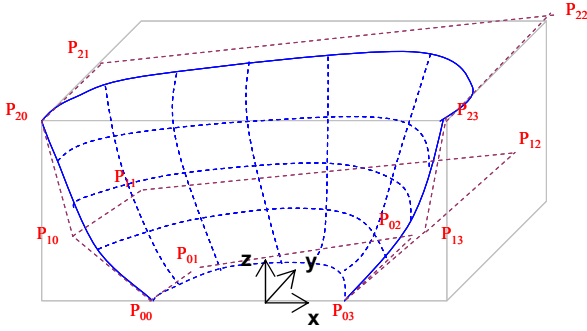


Figure 3 surface of degree (2,3) with its twelve control points

4. NUMERICAL RESULTS

4.1 Numerical Experiment

The solution of the inverse problem is considered with simulated data without and with noise (0.2%). Numerical computational has been performed by cast3M (<http://www-cast3m.cea.fr>) and Matlab. We use the optimisation toolbox to solve the identification problem. This toolbox calculates several times (number of function evolution) the function Cast3M to obtain the gradient.

Several numerical experiments have been performed in order to:

- Make the solution and convergence limits independent on computational parameters
- Choose a suitable number of sensors and their locations and simplify the experimental design procedure

For example, the temperature field $T(x, y, z; \Gamma)$ plotted in the figure 4 was obtained by solving the modelling equations (1)-(5) with a finite element approximation and the following numerical values:

$$h = 24.1 \times 10^{-4} \varepsilon T^{1.61} \text{ W/m}^2\text{K}, \quad \varepsilon = 0.9 \text{ (emissivity)}, \\ L_y = 60 \text{ mm}, \quad L_1 = 540 \text{ mm}, \quad L_2 = 60 \text{ mm}, \quad e = 3 \text{ mm}, \\ \rho_s = 7200 \text{ kg.m}^{-3}, \quad c_p = 550 \text{ J.Kg}^{-1}.\text{K}^{-1}, \quad \lambda_s = 50 \text{ W.m}^{-1}.\text{K}^{-1},$$

$T_f = 1450^\circ\text{C}$, $T_{imp} = 20^\circ\text{C}$, $u = 10 \text{ mm.s}^{-1}$ and the following control points $P_{00}^{\text{exp}}(-0.006, 0., 0.)$, $P_{01}^{\text{exp}}(-0.006, 0.0045, 0.)$, $P_{02}^{\text{exp}}(0.004, 0.0045, 0.)$, $P_{03}^{\text{exp}}(0.004, 0., 0.)$, $P_{10}^{\text{exp}}(-0.0075, 0., 0.0015)$, $P_{11}^{\text{exp}}(-0.0075, 0.008, 0.0015)$, $P_{12}^{\text{exp}}(0.005, 0.008, 0.0015)$, $P_{13}^{\text{exp}}(0.005, 0., 0.0015)$, $P_{20}^{\text{exp}}(-0.009, 0., 0.003)$, $P_{21}^{\text{exp}}(-0.009, 0.009, 0.003)$, $P_{22}^{\text{exp}}(0.006, 0.009, 0.003)$, $P_{23}^{\text{exp}}(0.006, 0., 0.003)$.

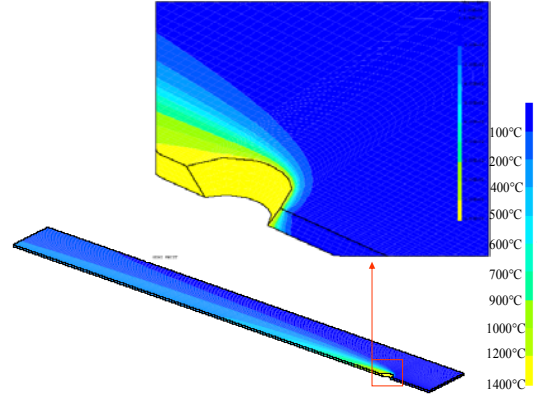


Figure 4 Temperature field in the solid obtained by numerical experiment

4.2 Results and Discussion

4.2.1 Influence of initial guess

The parameters vector to be found is:

$$X^{\text{exp}} = [P_{01y}^{\text{exp}}, P_{02y}^{\text{exp}}, P_{10x}^{\text{exp}}, P_{13x}^{\text{exp}}, P_{11y}^{\text{exp}}, P_{12y}^{\text{exp}}, P_{10z}^{\text{exp}}, P_{21y}^{\text{exp}}, P_{22y}^{\text{exp}}] \\ = (0.0045, 0.0045, -0.0075, 0.005, 0.008, \\ 0.008, 0.0015, 0.009, 0.009)$$

To perform the numerical procedure, the parameter coordinates are normalized in the range $[0, 1]$ by putting $P_{iky}^{\text{exp}} = \|P_{iky}^{\text{exp}}\| / P_y^{\text{norm}}$ with $P_y^{\text{norm}} = 0.006$ for all control points at the bottom of the work piece and $P_y^{\text{norm}} = 0.010$ for the other one, $P_{10x}^{\text{exp}} = \|P_{10x}^{\text{exp}} + 0.006\| / 0.003$, $P_{13x}^{\text{exp}} = \|P_{13x}^{\text{exp}} - 0.004\| / 0.002$, $P_{10z}^{\text{exp}} = \|P_{10z}^{\text{exp}}\| / e$. So, the transformed parameter vector to be found is:

$$X_{\text{norm}}^{\text{exp}} = (0.75, 0.75, 0.5, 0.5, 0.8, 0.8, 0.5, 0.9, 0.9).$$

Different initial guesses of the parameters vector are studied for a case using twelve sensors as shown in the table I and table II

For all of these five tests, the algorithm works well. Of course, we have the best solution when the initial guess approaches to the exact values. We show the evolution of estimated parameters in the case test N°5 (Figure 5)

Test No	Initial guess X^{input} ($P_{01y}, P_{02y}, P_{10x}, P_{13x}, P_{11y}, P_{12y},$ $P_{10z}, P_{21y}, P_{22y}$)	$\sqrt{S(\Gamma)}$ (°C)	Numb. of iterations
1	(0.1, 0.1, 0.1, 0.1, 0.1, 0.1, 0.1, 0.1, 0.1)	4.150	30
2	(0.2, 0.2, 0.2, 0.2, 0.2, 0.2, 0.2, 0.2, 0.2)	2.487	25
3	(0.5, 0.5, 0.5, 0.5, 0.5, 0.5, 0.5, 0.5, 0.5)	3.340	27
4	(0.9, 0.9, 0.9, 0.9, 0.9, 0.9, 0.9, 0.9, 0.9)	2.065	24
5	(0.9, 0.9, 0.9, 0.9, 0.5, 0.5, 0.8, 0.8, 0.8)	3.651	28

Table I Influence of initial guess

Test No	Number of iterations	Number of function evolution	Error estimated (%) $\frac{\ \Delta P\ }{\ P\ } = \frac{\sqrt{\sum (P_{ik}^{exp} - P_{ik}^{cal})^2}}{\sqrt{\sum (P_{ik}^{exp})^2}}$
1	30	510	12.81
2	25	402	9.73
3	27	410	13.68
4	24	426	13.25
5	28	483	14.41

Table II Error estimated

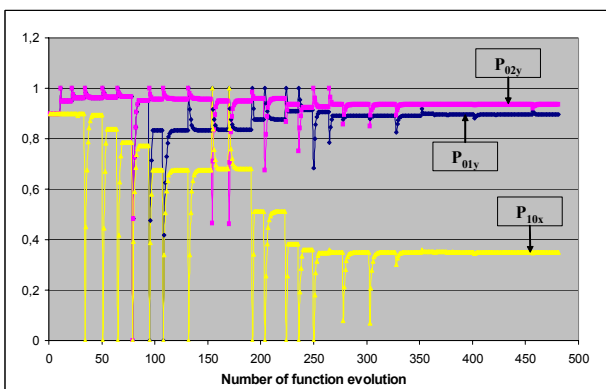


Figure 5a Parameter evolutions (Test N°5)

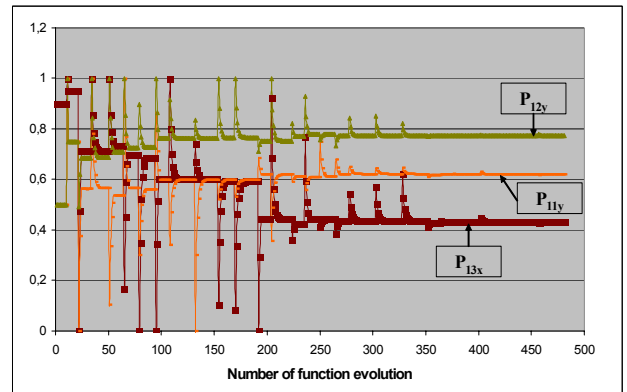


Figure 5b Parameter evolutions (Test N°5)

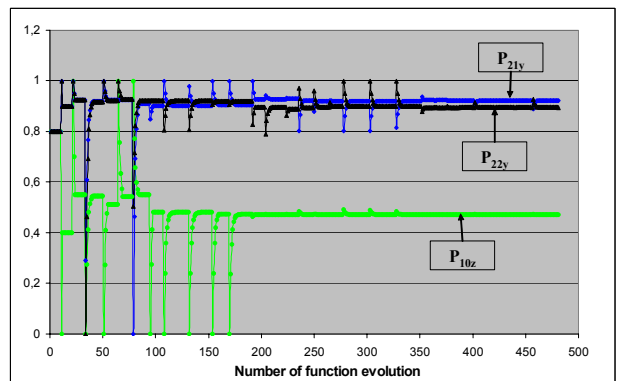


Figure 5c Parameter evolutions (Test N°5)

4.2.2 Influence of Sensor Number and Sensor Locations

The influence of both the number and the location of measurement points on the solution of the inverse problem are examined here. Two different sets of sensors respectively with $M = 10$; 12 for each set have been tested. The first one used five sensors on the top and five sensors on bottom of the work piece. The second one used six sensors on the top and six sensors on the bottom of the work piece. For each set, these sensors are located at $y_{tc}^{top} = 7.0mm$; $8.0mm$ and $y_{tc}^{bottom} = 5.0mm$; $5.5mm$ (Figure 6).

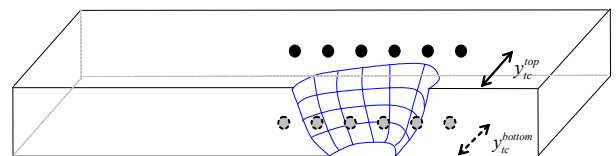


Figure 6 sensors location

The numerical procedure of these test cases starts from the same initial guess $X^{input} = (0.5, 0.5, 0.5, 0.8, 0.8, 0.8, 0.8, 0.8, 0.8)$.

It is important to notice from these results that the accuracy of the solution depends much more on the locations than on the number of sensors. Furthermore, for these cases studied here, the relative error of parameters estimation varies between 4,5% and 16%.

The best position corresponds to $y_{ic}^{top} = 7.0mm$ and $y_{ic}^{bottom} = 5.0mm$ with 10 sensors. This set of sensors is sufficiently distant from the weld pool to give the best information. In all cases the difference between the estimated temperature and the measured temperature is relatively small as shown in Table III and Table IV.

Sensor location			$\ Y^m - T(x_m, y_m, z_m)\ $ (°C)
x_m (mm)	y_m (mm)	z_m (mm)	
-6.0	8.0	3.0	5.21
-4.2	8.0	3.0	1.58
-2.4	8.0	3.0	3.72
-0.6	8.0	3.0	2.4
1.2	8.0	3.0	6.83
3.0	8.0	3.0	2.65
-4.0	5.5	0.	5.9
-2.8	5.5	0.	2.0
-1.6	5.5	0.	2.0
-0.4	5.5	0.	2.5
0.8	5.5	0.	6.0
2.	5.5	0.	2.09

Table III Comparison between measured and predicted temperatures (test case using 12 sensors)

Sensor location			$\ Y^m - T(x_m, y_m, z_m)\ $ (°C)
x_m (mm)	y_m (mm)	z_m (mm)	
-6.0	8.0	3.0	5.36
-3.75	8.0	3.0	2.22
-1.5	8.0	3.0	4.1
0.75	8.0	3.0	2.45
3.0	8.0	3.0	5.6
-4.0	5.5	0.	4.8
-2.5	5.5	0.	1.45
-1.0	5.5	0.	1.7
0.5	5.5	0.	4.2
2.0	5.5	0.	2.1

Table IV Comparison between measured and predicted temperatures (test case using 10 sensors)

5. CONCLUSIONS

This paper discussed a method to identify the shape of the phase change front in a quasi-steady state welding process. The problem is formulated as an inverse

geometry problem and solved iteratively, by minimizing a least square criterion. Fast convergence is achieved by modelling the shape of the interface using Bézier surfaces. The main advantage of this approach is due to the small number of parameter values to be identified, which consequently minimizes the number of required measurements. Moreover, this method is applicable for all welding processes: Tungsten Inert Gas (TIG); Metal Inert Gas (MIG); Metal Active Gas (MAG); Laser; Electrons Beam; Hybrid.

6. REFERENCES

1. A. Zacharia, S. David, J. Vitek, and T. Debroy, *Weld pool development during GTA and Laser Beam Welding of type 304 stainless steel*, part 11, experimental correlation, *Welding J.*, Vol. 68, (1989) pp. 510-519.
2. M. Thompson and J. Szekely, *The transient behavior of weld pool with a deformed free surface*, *Int. J. Heat Mass Transfer*, Vol. 32, (1989) pp. 1007-1019.
3. M. Katz and B. Rubinsky, *An inverse finite element technique to determine the change of interface location in one dimensional melting problem*, *Numer. Heat Transfer*, Vol. 7, (1984), pp. 269-283.
4. N. Zabaras and Y. Ruan, *A deforming finite element method analysis of inverse Stefan problem*, *Int. J. Numer. Meth. Eng.*, Vol. 28, (1989) pp. 295-313.
5. B. Rubinsky and A. Shitser, *Analytic solution to the heat equation involving a moving boundary with application to the change of phase problem : the inverse Stefan problem*, *ASME J. Heat Transfer*, Vol. 100, (1978) pp.300-304.
6. Y. F. Hsu, B. Rubinsky, K. Mahin, *An inverse Finite Element Method for Analysis of Stationary Arc Welding Processes*, *Journal of Heat Transfer*, Vol. 108, November 1986.
7. Nehad Al-Khadily, *Application of optimisation methods for solving inverse phase-change problems*, *Numerical Heat Transfer*, part B, 31: (1997) pp. 477-497.
8. N. Zabaras and K. Yuan, *Dynamic programming approach to the inverse Stefan design problem*, *Numer. Heat Transfer*, Vol. 26, (1994), pp. 97-107.
9. Nowak I., Andrzej J. Nowak, Louiz C. Wrobel : *Identification of phase change fronts by Bezier splines and BEM*. *Int. J. Therm. Sci.* 41 (2002) 492 – 499.
10. M. Necati Özisik, Helcio R. B. Orlande, *Inverse heat transfer fundamentals and applications*, (2000), Taylor & Francis.
11. D. D. Doan, F. Gabriel, Y. Jarny, P. Le Masson, *Utilisation des courbes de Bezier pour l'identification du front de fusion dans une opération de soudage*, *Congrès Français de Thermique, SFT 2006*, Ile de Ré, 16/05/2006 – 19/05/2006, France.

12. R. W. Lewis, K. Morgan, H. R. Thomas, K. N. Seetharamu, *The finite element method in heat transfer analysis*, Wiley, Chichester, 1996.
13. M. Zerokat, H. Power, L. C. Wrobel, *Heat and solute diffusion with a moving interface : A boundary element approach*, Int. J. Heat Mass Transfer, Vol. 41, (1998) pp. 2429-2436.
14. D. D. Doan, F. Gabriel, Y. Jarny, P. Le Masson, *Identification of a phase change front by Bezier splines for the heat transfer analysis of welding processes*, MCWASP, Opio, France, 2006.
- 15 N. Zabararas, S. Mukherjee, and O. Richmoud, *An analysis of inverse heat transfer problems with phase changes using an integral method*, ASME J. Heat Transfer, Vol. 110, (1988) pp. 554-561.